

Intermodal Modulation Instability and Four-Wave Mixing in Graded-Index Few-Mode Fibers

A. Bendahmane¹, R. Dupiol^{1,2}, K. Krupa³, A. Tonello², J. Fatome¹, M. Fabert², B. Kibler¹, T. Sylvestre⁴,
A. Barthelemy², V. Couderc², S. Wabnitz^{1,3}, and G. Millot^{1,*}

¹Université Bourgogne Franche-Comté, ICB, UMR CNRS 6303, 9 Avenue A. Savary, 21078 Dijon, France

²Université de Limoges, XLIM, UMR CNRS 7252, 123 Avenue A. Thomas, 87060 Limoges, France

³Università di Brescia, Dipartimento di Ingegneria dell'Informazione and INO-CNR, via Branze 38, 25123 Brescia, Italy

⁴Université Bourgogne Franche-Comté, Institut FEMTO-ST, UMR CNRS 6174, 15B Avenue des Montboucons, 25030 Besançon, France

*guy.millot@u-bourgogne.fr ;

Abstract: By controlling pump modes injected in the normal dispersion regime of few-mode graded index optical fiber, we investigated intermodal noise-seeded modulation instability and generation of highly-detuned cascaded intermodal four-wave mixing sidebands. © 2018 The Author(s)

OCIS codes: (190.4370) Nonlinear optics, fibers; (190.4410) Nonlinear optics, parametric processes; (190.4380) Nonlinear optics, four-wave mixing.

1. Introduction

In recent years, an intensive research activity on multimode fibers has led to the observation of a series of complex and novel nonlinear spatiotemporal phenomena such as: multimode solitons, geometric parametric instability, supercontinuum generation, and self-induced beam cleaning [1-4]. Most of these observations involved highly multimode fibers. In this work, we investigate the case of a graded-index few-mode fiber (GRIN-FMF) that exhibits a large normal dispersion at 1064 nm. By controlling the spatial modes excited at the fiber input, we experimentally observed and theoretically explained complex nonlinear frequency conversion processes, associated with intermodal modulation instability (IM-MI) or intermodal four-wave mixing (IMFWM). Particularly, a new cascaded IMFWM process leads to the generation of the most detuned parametric frequency sidebands observed to date in a FMF.

2. Bimodal Modulation instability in a GRIN-FMF

The fiber used in our study is a GRIN-FMF that exhibits a central parabolic index shape of the form: $n^2(\rho) = n_0^2 [1 - 2\Delta (\rho/R)^2]$, with $n_0 = 1.464$, $R = 11 \mu\text{m}$, $\Delta = 0.0089$. This fiber has been specially designed, in order to support two groups of modes at 1550 nm and four modes (LP01, LP12, LP11 and LP02) at 1064 nm (Fig. 1(a)).

Nonlinear processes taking place in a multimode fiber highly depend on which modes are excited by the pump beam. To simplify the analysis, we first limit ourselves to only two groups of injected modes, and studied the conditions for observing MI sidebands [5]. By analyzing the stability of stationary solutions, we determined that among the five pairs of possible modes, only three of them (LP01-LP11, LP01-LP02, LP11-LP21) may undergo MI. The associated gain spectra are calculated and represented in Fig. 1(a). They exhibit a zero cut off frequency, similar to the case of pure scalar MI. Notice that the two mode pairs LP01-LP11, and LP01-LP02, have the same gain. We also found that, for high pump powers, MI sidebands are composed by a mix of two spatial modes. Hence the MI process involves a nonlinear interaction of six waves, and can no longer be interpreted as a simple FWM process.

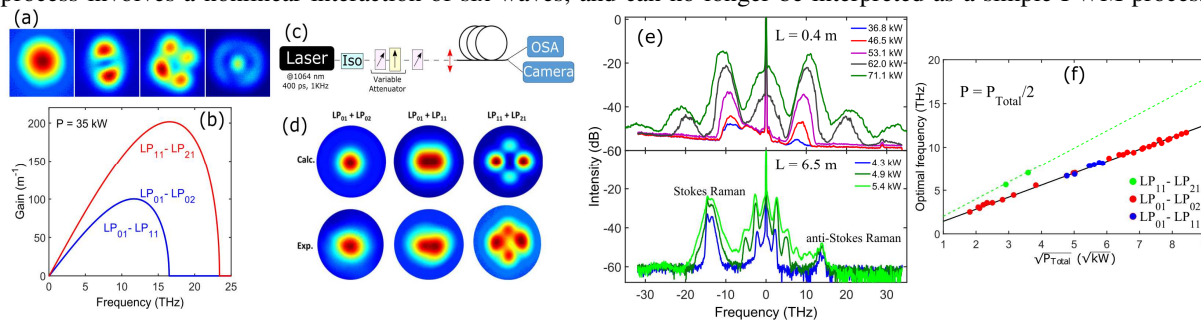


Fig. 1 (a) Spatial modes supported at 1064 nm. (b) Theoretical gain spectra for the three unstable pairs of modes. (c) Calculated (Calc.) and measured (Exp.) output spatial profile for different combinations of modes. (d) Experimental setup. (e) Experimental spectra recorded at different input total peak powers in the case of the excitation of the pair of modes (LP01-LP02). (f) Power dependence of the optimal frequency. Experimental measurements (dots) for the different groups of modes are compared with linear stability analysis results (lines).

To experimentally observe IM-MI, we used the experimental setup represented in Fig. 1(c). By finely adjusting the injection conditions, we were able to selectively excite each of the three pairs of unstable modes (Fig. 1(d)). Figure 1(e) shows MI spectra recorded with the excitation of the pair of modes LP01-LP02, for input peak powers

ranging from 36.8 to 71.1 kW. To acquire spectra at lower pump powers, longer fiber lengths were used. The MI spectra exhibit a strong power dependence, with an optimal (peak gain) frequency scaling as the square root of power (dots, Fig. 1(f)), in excellent agreement with a theoretical bimodal-MI model (lines). Moreover, the two pairs of modes LP01-LP11 and LP01-LP02 have identical optimal frequencies, in agreement with gain curves.

3. Highly-detuned cascaded intermodal four-wave mixing

In a second set of experiments, we used a 1-m-long piece of the same GRIN-FMF. This time, the pump beam was carefully adjusted to mainly excite the LP01 mode, in order to avoid any IM-MI. Figure 2(a) shows a set of spectra recorded while increasing the pump peak power from 44 kW to 80 kW. We first observed the generation of a narrowband far-detuned sideband located at 625.2 nm (198 THz from the pump), due to intermodal phase matching. When increasing the pump power up to 50 kW, the conversion efficiency into this sideband increased, and we observed new far-detuned spectral peaks ranging between 400 and 550 nm. Also, a broad Raman continuum of 200 nm bandwidth developed around the pump.

Spectral and spatial measurements combined with analytical estimates based on ref. [6] allowed us to determine that the pump energy at 1064 nm is essentially transferred to the first and second anti-Stokes (625.2 and 555.2 nm), owing to IMFWM. The 625.2 nm component then acts as a *secondary pump*, and generates all the anti-Stokes peaks below 532 nm along with their corresponding Stokes peaks (see Fig. 2(c)). The spectral shifts (from the secondary pump) of these cascaded visible parametric sidebands can be predicted by the analytical formula by Mafi et al. [6]: $f_n^2 \approx n\sqrt{2\Delta}/(2\pi^2 R\beta_2)$ (n is the sideband order), and are represented by vertical lines in Fig. 2(b). These positions are found in very good agreement with the experimental values. The component at 442 nm (blue arrow, Fig. 2(b)) is generated due to *intramodal FWM* between the main pump (1064 nm) and the secondary pump (625 nm) (Fig. 2(c)).

To confirm our physical interpretation, we numerically solved the (3+1)D nonlinear Schrödinger equation [4,7]. Two separate simulations were done for a pump wavelength set at either 1064 nm or 625 nm. We obtained idler wavelengths which are in remarkable agreement with both analytic calculations [7] and experimental observations. Hence, we validated the secondary pump mechanism that is summarized in Fig. 2(c).

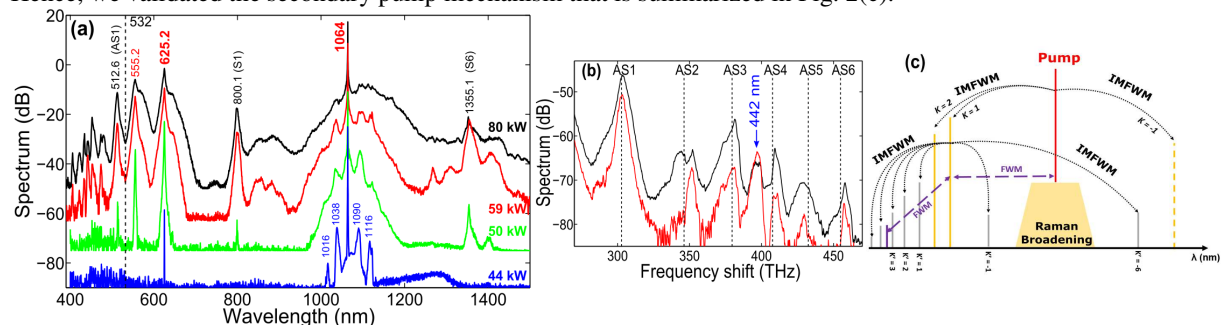


Fig. 2 (a) Output spectra recorded for a pump peak power of 44 kW (blue), 50 kW (green), 59 kW (red), and 80 kW (black). (b) Zoom on the visible part of the 59 and 80 kW spectra. The vertical dashed lines indicate the calculated IMFWM frequencies for a secondary pump at 625.2 nm propagating in the LP01 mode. The blue arrow indicate intra-modal FWM implying the main pump. (c) Schema summarizing the processes.

4. Conclusion

We reported the experimental observation of bimodal MI in a normally dispersive GRIN few-mode fiber. We also identified a new cascaded intermodal FWM mechanism, inducing the generation of a series of spectral sidebands ranging from 405 nm up to 1355 nm, the largest frequency range observed to date in a FMF. These findings are relevant for the development of new photonic devices such as parametric amplifiers and laser sources that expand the range of laser light emission via nonlinear frequency conversion processes. The results concerning IM-MI open a new route for the generation of high-repetition rate vector soliton trains.

5. References

- [1] L. G. Wright et al., "Controllable spatiotemporal nonlinear effects in multimode fibres," *Nature Photonics* 9, p. 306-310 (2015).
- [2] S. Longhi, "Modulational instability and space time dynamics in nonlinear parabolic-index optical fibers," *Opt. Lett.* 28, p. 2363 (2003).
- [3] K. Krupa et al., "Observation of geometric parametric instability induced by the periodic spatial self-imaging of multimode waves," *Phys. Rev. Lett.* 116, p. 183901 (2016).
- [4] K. Krupa et al., "Spatiotemporal characterization of supercontinuum extending from the visible to the mid-Infrared in multimode graded-Index optical fiber," *Opt. Lett.* 41, p. 5785 (2016).
- [5] R. Dupiol et al., "Intermodal modulational instability in graded-index multimode optical fibers," *Opt. Lett.* 42, 3419-3422 (2017).
- [6] E. Nazemosadat et al., "Phase matching for spontaneous frequency conversion via four-wave mixing in graded index multimode optical fibers," *J. Opt. Soc. Am. B* 33, p. 144 (2016).
- [7] R. Dupiol et al., "Far-detuned cascaded intermodal four-wave mixing in a multimode fiber," *Opt. Lett.* 42, 1293-1296 (2017).